



REGULAR ARTICLE

Efficient dye-sensitized solar cell based on a new porphyrin complex as an inorganic photosensitizer

AZAM NASIRIAN*, VALIOLLAH MIRKHANI*, MAJID MOGHADAM*,
SHAHRAM TANGESTANINEJAD and IRAJ MOHAMMADPOOR-BALTORK
Catalysis Division, Department of Chemistry, University of Isfahan, 81746-73441 Isfahan, Iran
E-mail: aazamnasirian@gmail.com; mirkhani@sci.ui.ac.ir; moghadamm@sci.ui.ac.ir

MS received 15 December 2019; revised 14 February 2020; accepted 17 February 2020, corrected publication 2020

Abstract. The synthesis of new porphyrin complexes that can absorb light in a broad range of the spectrum is very important for getting a high efficiency in dye-sensitized solar cells. The primary reason for using these complexes is good photophysical characteristic like good absorption and high quantum efficiency. Most of the metal porphyrin shows good photophysical characteristics with changing their ligands. In this work, the synthesis of a new Zn-porphyrin complex, that has a good spectral and electrochemical characteristic, is reported. Then, this complex is used as a dye in dye-sensitized solar cells, using titanium dioxide as a semiconductor. The application of this complex in a dye-sensitized nanocrystalline TiO₂ solar cell has indicated a short circuit density of 11.60 mA, an open circuit potential of 0.65 V with an overall efficiency of 5.33%. The overall conversion efficiency of this system is due to the efficient electron injection into the conduction band during light absorption.

Keywords. Dye-sensitized solar cell; sensitizing dye; titanium dioxide; electron transfer; Zn-porphyrin complex.

1. Introduction

Dye-sensitized solar cells (DSSCs) are cheap and they are a good option instead of p-n junction cells.¹ These days the manufacturing of DSSCs has picked up interest because of the low cost and simple fabrication of them comparing to silicon solar cells.² DSSCs are manufactured by the sandwich arrangement of two electrodes; anode electrode that consists of TiO₂ or SnO₂ thin layer coated with dye, and platinum (Pt) that used as a coated counter electrode. The space between two electrodes is filled with a redox pair electrolyte, such as I⁻/I₃⁻.³⁻⁶ Various factors influence the photovoltaic efficiency of DSSCs. For improving the efficiency of the DSSCs, their fragments such as semiconductor, dye, and electrolyte are used to improve the results in different works. The mesoporous TiO₂ thin film and sensitizers have an important role in improving solar cell efficiency. DSSCs is a photoelectrochemical solar cell that consists of complex photoexcited reactions, electro-chemical

reactions, electron transports at different interfaces in the cell, photocatalytic reaction. The interfacial energetics and kinetics are important in DSSCs because this information allows us to know how to reduce energy loss and achieve high efficiency, both of which are strongly dependent on the precise determination of energy levels and the complete realization of reaction kinetics at cell interfaces.³ The most important characteristic of DSSC is using different sensitizers, such as transition metal complexes, phthalocyanines, organic dyes, and metalloporphyrins. For having high efficiency in DSSCs, the sensitizer should be panchromatic. It can be justified with the high absorption of photons in the broad region of the spectrum. Also, it maintains a thermodynamic driving force for the regeneration of dye and the injection of the electron.^{7, 8} Porphyrin has two absorption bands in the UV-vis spectrum: Soret and Q-bands. These bands appear in blue and red regions, respectively. With changing the ligand of these complexes, these bands can be shifted and thus increase the amount of photon

*For correspondence

absorption and an increased amount of efficiency in DSSCs. The design of new porphyrins while changing the substituents, can help us modify photophysical and photochemical characteristics of these compounds which imitate photosynthetic solar energy transfer *via* changing photon energy to chemical potential.^{9–13} Thus, porphyrins have attracted attention because of some advantages such as high molar extinction coefficient, especial structure, simple synthesis method, low toxicity and low cost.^{14–19} Recently, Yella and co-workers¹⁸ used a cobalt electrolyte with a porphyrin dye as a photosensitizer. The efficiency of this solar cell was 12.3%. Also, porphyrin photosensitizers in DSCs were made by Yeh and Imahori's groups.^{20–22} Under the optimized condition, the efficiency of 4.1% was obtained. Based on previous work on different functionalized porphyrins for DSSCs by Grätzel and co-workers,¹⁸ recently, Insuasty and co-workers synthesized new systems containing a diphenylamine-Zn (II)-porphyrin with a vinylfluorene as the π -bridge, and cyanoacrylic acid, or dicyanorhodanine as the anchoring acceptors groups with a conversion efficiency of 5.56 and 4.13%.²³ So, based on these works, we have designed and synthesized a new system containing a Zn (II)-porphyrin complex with aminophenyl electron donor groups as a dye for DSSC. So in this work, we report the synthesis, characterization as well as optical, electronic and photovoltaic properties of the novel Zn (II) porphyrin sensitizer and its application as a potential sensitizer for the fabrication of photovoltaic solar cell with I^-/I_3^- electrolyte and with the efficiency of 5.33%.

2. Experimental

2.1 Materials

All solvents were dried and distilled before use. Most commercial reagents were used without further purification. All reagents for the chemical synthesis were purchased from Sigma-Aldrich chemical company. ¹H and ¹³C NMR spectra were recorded in CDCl_3 or DMSO solvents by a Bruker– Avance 400 NMR Spectrometer. UV–Vis spectra were obtained by a JASCO V–670 UV–Vis Spectrophotometer (190–2700 nm). FT–IR spectra were obtained by a JASCO, FT/IR–6300 instrument (400–4000 cm^{-1}).

2.2 Synthesis of 1, 3-dioctyloxybenzene

Compound 1, 3-dioctyloxybenzene was synthesized according to the reported procedure.^{18, 24} First, resorcinol (11 g, 0.1 mol) was added to a flask and then 1-bromooctane (69.6 mL, 0.4 mol) and K_2CO_3 (69 g, 0.5 mol) were added respectively. Then the reaction mixture was refluxed in 500

mL dry acetone for 4 days. Then, the solvent was removed under reduced pressure. Finally, the compound was extracted with EtOAc. The organic layer was washed with water and dried over anhydrous MgSO_4 . Then, the solvent was removed under reduced pressure and the product was purified by column chromatography with hexane as eluent to give 1,3-di(octyloxy)benzene. The sample was characterized by FT–IR and ¹H NMR spectroscopy. ¹H NMR (CDCl_3 , 400 MHz) δ (ppm) = 7.09 (t, $J=8.4$ Hz, 1H), 6.29 (m, 3H), 3.87 (t, $J=6.4$ Hz, 4H), 1.76 (m, 4H), 1.58 (m, 4H), 1.32–1.28 (m, 16H), 0.88 (t, $J=7.6$ Hz, 6H).

2.3 Synthesis of 2-(bromomethyl)-1, 3-bis(octyloxy) benzene (compound 1)

Concentrated HBr was added to 1, 3-dioctyloxybenzene (9.15 g) and paraformaldehyde (5 g) and the mixture was stirred at room temperature for 48 h. Then, the reaction mixture was filtered and the precipitate was washed with NaHCO_3 and water, respectively, and then, the dried under vacuum. The sample was purified by column chromatography using a 1:1 mixture of hexane and dichloromethane as eluent. The product was characterized by FT–IR and NMR spectroscopy.

2.4 Synthesis of 5, 10, 15, 20-tetrakis (4-aminophenyl) porphyrinato zinc (II), [Zn(TNH₂PP)] (compound 2)

Compound $\text{H}_2\text{TNH}_2\text{PP}$ was synthesized according to the procedure reported in the literature.²⁵ First, a solution of $\text{H}_2\text{TNH}_2\text{PP}$ (0.5 g) and $(\text{Zn}(\text{OAc})_2 \cdot 2\text{H}_2\text{O})$ (1.4 g) dimethylformamide (100 mL) was refluxed for 3 h. Then, the reaction mixture was filtered after 3 h at room temperature. The product was washed with distilled water and acetone respectively and then dried. After recrystallization of the product a mixture of dichloromethane-methanol, the collected product was purified in the silica-gel column chromatography with dichloromethane as eluent. The first band was collected and finally, the solvent was removed under reduced pressure.²⁶ The complex was characterized by FT–IR, UV–vis, and NMR spectroscopic techniques.

2.5 Synthesis of compound 4

Zn-porphyrin complex $[\text{Zn}(\text{TNH}_2\text{PP})]$ (compound 2) (0.16 g), and 2-(bromomethyl)-1,3-bis(octyloxy)benzene (compound 1) (0.279 g) was poured in a 100 mL single-aperture flask, and triethylamine (3 mL) and toluene (50 mL) were then added to it, and the mixture was heated at 80 °C and refluxed in darkness for 72 h. The mixture was cooled to room temperature and it was filtered after cooling. The filter product was washed several times with Acetonitrile and then dried under vacuum at room temperature. The complex

was characterized by FT-IR, UV-Vis, and NMR spectroscopic techniques.

2.6 Synthesis of copper (I) iodide

Cu(NO₃)₂ · 2H₂O (0.101 g), and H₂O (4 mL) were poured in a 25 mL single-aperture flask, and the mixture was stirred. Then Ascorbic acid (0.072 g) was added to the solution and finally, NaI (0.063 g) dissolved in 2 mL H₂O was added to the previous solution while stirring. Then, the white precipitate of CuI was filtered. The filter product was washed several times with Ethanol and Ether, respectively and dried at room temperature. Then it was used for synthesis in the next step.

2.7 Synthesis of 3-[4-benzoic acid]pentane-2,4-dione (compound 3)

The 3-[4-benzoic acid]pentane-2,4-dione was synthesized according to the procedure reported in the literature.^{27, 28} First, a mixture of 2,4-pentanedione (4.5 mmol), 4-iodobenzoic acid (1.5 mmol), K₂CO₃ (7.5 mmol), CuI (0.15 mmol) and L-proline (0.3 mmol) and dry DMSO solvent (15 mL) were added to the three-necked flask under stirring and reaction mixture was heated at 90 °C under nitrogen atmosphere for 24 h. The reaction solution was allowed to cool and the cooled solution was poured into 1 M HCl and extracted with ethyl acetate (3 × 100 mL). The organic layer was dried over Na₂SO₄ and the solvent was removed by reduced pressure. The crude was dried under vacuum for 24 h. The crude oil was purified by silica gel column chromatography, using a mixture of hexane/ethyl acetate (1:1) as eluent.

2.8 Synthesis of dye (compound 5)

3-[4-benzoic acid]pentane-2,4-dione (compound 3) (0.056 g) and Dichloromethane (CH₂Cl₂) (5 mL) were added to a 50 mL, one-necked flask under stirring. Thionyl chloride (4 mL) was added dropwise to the solution. The solution was refluxed for 3 h by stirring. After cooling the solution to room temperature, nitrogen gas is passed through the solution until volatiles removed from the solution. Then Dichloromethane (CH₂Cl₂) (5 mL) and *N,N*-Diisopropylethylamine (0.040 g) were added to the reaction solution and was stirred for 10 min at room temperature. After removing volatiles and white vapors from the reaction flask, compound 4 (0.453 g) was added to CH₂Cl₂ (10 mL), under stirring was added to the mixture. The mixture was refluxed for 24 h by stirring. The cooled solution was poured into an equal amount of water and extracted with ethyl acetate three times. The organic layer was washed with an aqueous saturated solution of NaHCO₃ and then dried over Na₂SO₄.

After removal of the volatile materials, the collected oil crude was purified by column chromatography on silica gel with Ethyl acetate and Methanol (1%) as eluent and the first band was collected as product. Finally, the solvent was evaporated and the complex was separated. The zinc porphyrin complex dye (compound 5) was characterized by ESI-MS, CHN analysis, FT-IR, and NMR spectroscopic techniques. ESI-MS: m/z /2, (ZnC₁₂₅H₁₅₆N₈O₉)/2, Found: 990.125, Calculate: 990.0075.

This complex was used as a dye for the fabrication of dye-sensitized solar cell, and the current-voltage curve and efficiency of this cell was measured.

2.9 TiO₂ thin film preparation

TiO₂ paste (average particle size about 13 nm) was purchased from Solaronix Company. TiO₂ thin film was prepared by a doctor blade method. To obtain a mesoporous film of uniform thickness, we used Scotch tape and a glass rod to spread a drop of viscous TiO₂ suspension onto a microscope glass slip. After removal of the tape and drying in air at room temperature for about 1 h, it was sintered at 550 °C for 35 min to form a transparent TiO₂ thin film. Dye sensitization of the TiO₂ film was carried out by soaking the still hot (80 °C) film in the synthesized Zn porphyrin complex (0.5 mM in CH₂Cl₂ solvent) and incubated at room temperature for two days. After finishing the sensitization procedure, the film was rinsed with ethanol three times to remove the non-attached dye and finally sealed. Dye-sensitized films were prepared and kept in dark place before measurement.

2.10 Cell assemble

A solar cell was manufactured using the dye attached TiO₂ film as a working electrode and a second conducting glass coated with chemically deposited platinum from 0.05M hexachloroplatinic acid as a counter electrode. The two electrodes were covered with the transparent film of Surlyn polymer and were tightly held and heated (100 °C) around the Surlyn to seal and attach two electrodes. A thin layer of electrolyte solution containing I⁻/I³⁻ couple was pervaded into the electrode between spaces from the counter electrode side through a very tiny hole. Then, the drilled hole was covered with a microscope cover slide and Surlyn to avoid leakage of the electrolyte solution. The current-voltage (I-V) curves of the dye-sensitized solar cells were measured with μ-Autolab type III (Ecovchemie, Utrecht, the Netherlands) controlled by a microcomputer with Nova 1.7 software, under the illumination of 100 mW cm⁻² using the solar simulator (Luzchem, V 1.2) equipped with a water-based IR filter.

3. Results and Discussion

The preparation route for dye is shown in Figure 1.

Compound 1,3-dioctyloxybenzene was characterized by FT-IR and NMR methods. The C-O-C groups appear in the region of 1153 and 1181 cm^{-1} . The C=C bands and aromatic rings appear in 1457 cm^{-1} and 1591 cm^{-1} . The aliphatic and aromatic C-H stretching bands appear in 2860 and 2955 cm^{-1} , respectively.

^1H NMR (CDCl_3 , 400 MHz) δ (ppm) = 7.09 (t, $J=8.4$ Hz, 1H), 6.29 (m, 3H), 3.87 (t, $J=6.4$ Hz, 4H), 1.76 (m, 4H), 1.58 (m, 4H), 1.32–1.28 (m, 16H), 0.88 (t, $J=7.6$ Hz, 6H).

Compound **1** was characterized by FT-IR and NMR methods. The C-Br bands appear in the region 700–900 cm^{-1} . The intense absorption bands at 1153 and 1181 cm^{-1} correspond to C-O-C groups. The C=C bands and aromatic rings appear in 1457 cm^{-1} and

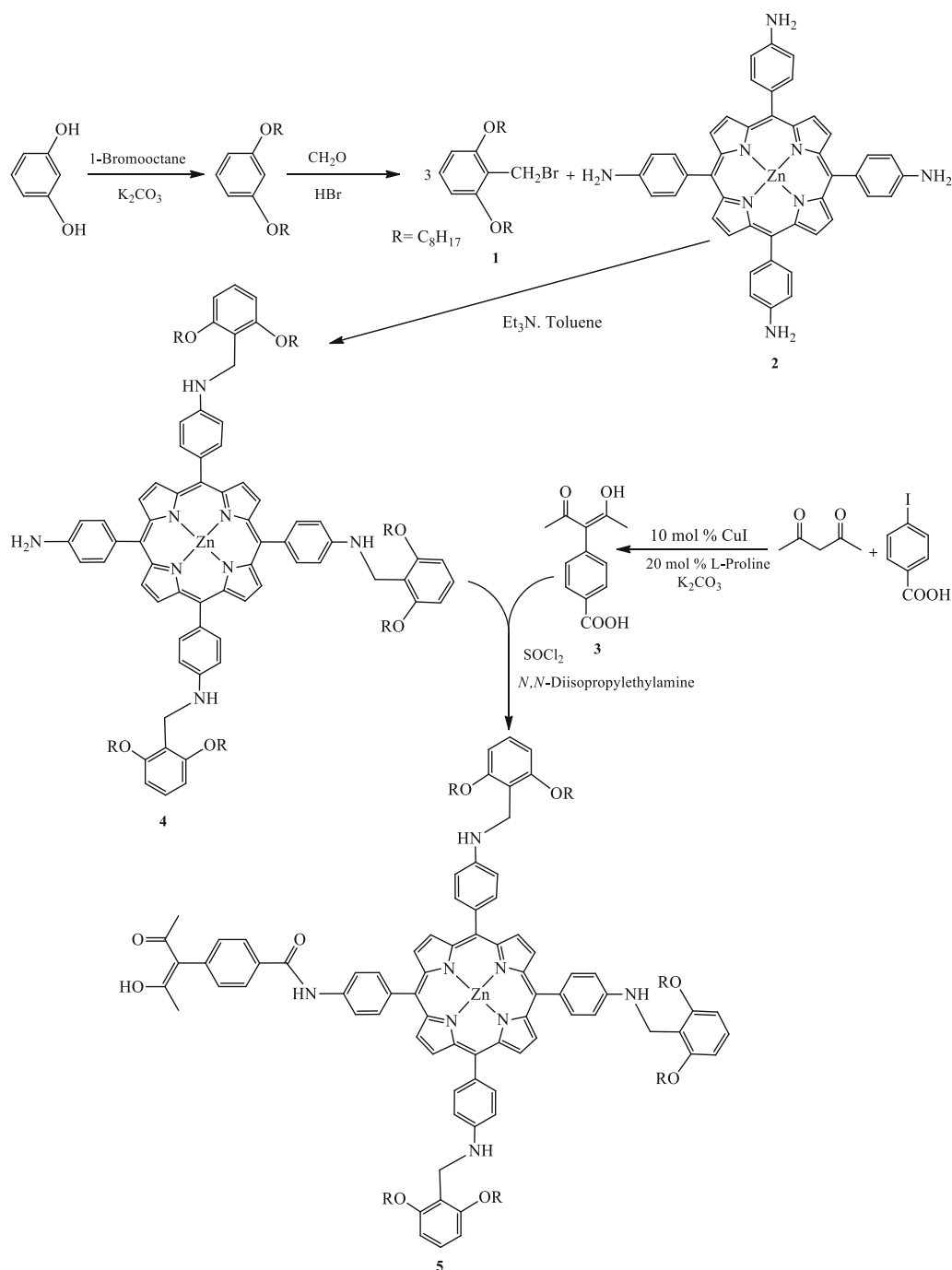


Figure 1. The preparation route for dye synthesis.

1591 cm^{-1} . The absorption bands at 2860 cm^{-1} and 2955 cm^{-1} are assigned to the aliphatic and aromatic C–H stretching bonds, respectively.

^1H NMR: (CDCl_3 , 400 MHz) δ (ppm) = 0.93 (t, $J=6.4$ Hz, 6H), 1.32–1.37 (m, 16H), 1.50–1.53 (m, 4H), 1.84–1.87 (m, 4H), 3.77 (t, $J=6.4$ Hz, 4H), 4.55 (s, 2H), 6.17 (d, $J=8.4$ Hz, 2H), 7.07 (t, $J=8$ Hz, 1H).

^{13}C NMR: (CDCl_3 , 100 MHz) 155.71 (C_a), 130.89 (C_b), 121.44 (C_d), 106.60 (C_c), 68.76 (C_f), 31.92 (C_k), 29.64 (C_g), 29.64 (C_i), 29.36 (C_j), 26.14 (C_h), 22.72 (C_l), 14.15 (C_e), 14.1 (C_m).

In the FT–IR spectrum of compound **2**, the absorption bands at 797 and 1516 cm^{-1} are due to the N–H Out-of-plane bending vibrations and scissor-like bending vibrations, respectively. The C=N and C=C stretching bands of metalloporphyrin appear at 1663 cm^{-1} . The absorption bands at 2850 and 2918 cm^{-1} are due to the C–H stretching bonds. The appeared band at 3368 cm^{-1} is assigned to NH of the NH_2 group in the porphyrin ring.

^1H NMR: (CDCl_3 , 400 MHz) δ (ppm) = 3.73 (s, 8H, H^a), 6.78 (d, $J=8$ Hz, 8H, H^b), 6.98 (d, $J=8$ Hz, 8H, H^d), 7.58 (d, $J=8$ Hz, 8H, H^c).

^{13}C NMR: (CDCl_3 , 100 MHz) 148.51 (C_a), 139.50 (C_f), 130.50 (C_d), 129.33 (C_c), 123.43 (C_e), 121.41 (C_g), 115.70 (C_b).

The UV–vis spectrum of compound **2** in DMF exhibits the typical metal to ligand charge transfer (MLCT) transition of the Zn porphyrin complex at $\lambda_{\text{max}} = 436$ nm, 568 nm and 614 nm (Figure 2).

In the FT–IR spectrum of compound **4**, the absorption bands at 796 and 1506 cm^{-1} are due to the N–H Out-of-plane bending vibrations and scissor-like bending vibrations, respectively. The C=N and C=C stretching bands of metalloporphyrin appear at 1610 cm^{-1} .

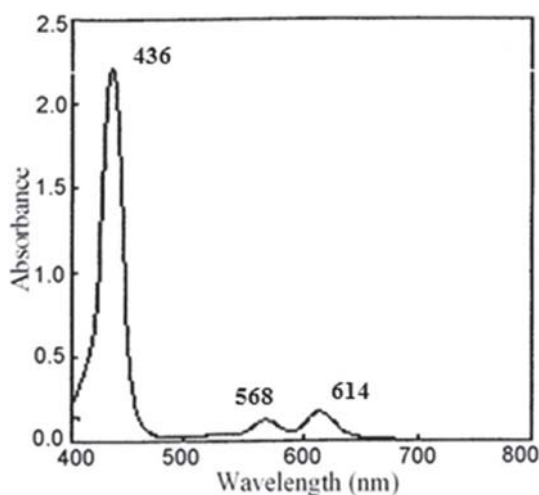


Figure 2. UV–Vis spectrum of Zn porphyrin complex (compound **2**) in DMF.

The absorption bands at 2864 and 2924 cm^{-1} are due to the C–H stretching bonds. The appeared bands at 3390 and 3438 cm^{-1} are assigned to NH of NH_2 groups in the porphyrin ring.

^1H NMR (CDCl_3 , 400 MHz): δ (ppm) = 0.88 (t, $J=6.8$ Hz, 18H, H_h), 1.35 (m, 48H, H_c , H_d , H_e , H_f), 1.45 (m, 12H, H_g), 1.68 (m, 12H, H_b), 3.69 (d, $J=8$ Hz, 6H, H_i), 3.84 (t, $J=4$ Hz, 12H, H_a), 4.29 (t, $J=4$ Hz, 3H, H_m), 4.32 (s, 2H, H_z), 5.29 (d, $J=0.8$ Hz, 2H, H_p , H_u), 5.82 (d, $J=1.2$ Hz, 2H, H_s , H_q), 6.36 (d, $J=7.6$ Hz, 6H, H_j , H_k), 6.44 (d, $J=6$ Hz, 7H, H_n , H_r), 6.47 (d, $J=6.4$ Hz, 1H, H_t), 6.65 (d, $J=4$ Hz, 2H, H_v , H_w), 6.78 (dd, $J=6$, 14 Hz, 3H, H_j), 7.15 (d, $J=2$ Hz, 6H, H_o), 7.71 (d, $J=5.2$ Hz, 2H, H_y), 8.02 (d, $J=1.6$ Hz, 2H, H_x).

^{13}C NMR: (CDCl_3 , 100 MHz) 154.76 (C_i), 150.36 (C_l), 145.73 (C_z , C_n), 135.92 (C_s), 130.91 (C_u), 127.77 (C_y , C_p , C_k , C_q), 121.46 (C_v , C_x), 116.14 (C_r , C_z), 113.16 (C_1 , C_o), 105.91 (C_j), 97.68 (C_w), 68.77 (C_a), 31.93 (C_f), 29.5 (C_b , C_d , C_e), 26.16 (C_c , C_m), 22.14 (C_g), 14.16 (C_h).

Also, CHN analysis was carried out to determine the presence of ligand and metal in the porphyrin complex (compound **4**). CHN analysis of compound obtained: Anal. Calc. For $\text{ZnC}_{113}\text{H}_{146}\text{N}_8\text{O}_6$: C, 76.38; H, 8.22; N, 6.31. Found: C, 76.28; H, 8.26; N, 6.27%.

The FT–IR spectrum of compound **3** showed an intense absorption band at 1686 cm^{-1} due to the presence of the C=O functional group, while the band observed at 1606 cm^{-1} corresponds to the C=C bond. The stretching vibration of carboxylic acid O–H and the other OH groups appear as a very broad band in the region 2800–3400 cm^{-1} , centered at about 3000 cm^{-1} . The absorption bands at 2999 cm^{-1} and 3070 cm^{-1} is assigned to the C–H bonds. These observations proved the structure of compound **3**.

^1H NMR (CDCl_3 , 400 MHz) (100% enol form) δ (ppm) = 16.74 (s, 1H, OH), 8.15 (d, $^3J_{\text{H-H}} = 8$ Hz, 2H, CH_{Ar}), 7.33 (d, $^3J_{\text{H-H}} = 8$ Hz, 2H, CH_{Ar}), 1.91 (s, 6H, CH_3).

^{13}C NMR (CDCl_3 , 100 MHz): 190.7 (C–OH), 171.1 (COOH), 142.8 (C_{Ar}), 131.4 (CH_{Ar}), 130.7 (CH_{Ar}), 128.6 (C_{Ar}), 114.5 (C_{Enol}), 24.2 (CH_3).

In the FT–IR spectrum of compound **5** (dye), the absorption bands at 800 and 1514 cm^{-1} are due to the N–H Out-of-plane bending vibrations and scissor-like bending vibrations, respectively. The C=N and C=C stretching bands of metalloporphyrin appear at 1594 and 1674 cm^{-1} . The stretching bands of the C–H appear in 2853 and 2923 cm^{-1} . The appeared band at 3314 cm^{-1} is assigned to NH of NH_2 groups in the porphyrin ring. The stretching vibration of OH group appears as a very broadband and strong in the region 3000–3700 cm^{-1} .

^1H NMR (CDCl_3 , 400 MHz) δ (ppm) = 0.82 (t, J = 6.8 Hz, 18H, H_h), 1.21 (m, 48H, H_c , H_d , H_e , H_f), 1.40 (m, 12H, H_g), 1.70 (m, 12H, H_b , H_c), 2.26 (s, 3H, H_d), 3.685 (d, J = 7.6 Hz, 6H, H_i), 4.00 (t, J = 4.4 Hz, 12H, H_a), 4.31 (t, J = 4 Hz, 3H, H_m), 5.29 (d, J = 0.8 Hz, 2H, H_p , H_u), 5.82 (d, J = 1.2 Hz, 2H, H_s , H_q), 6.23 (d, J = 7.6 Hz, 6H, H_i , H_k), 6.37 (d, J = 12 Hz, 7H, H_n , H_r), 6.48 (d, J = 6.4 Hz, 1H, H_l), 6.65 (d, J = 4 Hz, 2H, H_v , H_w), 6.78 (dd, J = 6, 14 Hz, 3H, H_j), 7.11 (d, J = 2.4 Hz, 6H, H_o), 7.71 (d, J = 5.2 Hz, 2H, H_y), 8.02 (d, J = 1.6 Hz, 2H, H_x), 8.28 (d, J = 8 Hz, 2H, H_b), 8.45 (d, J = 7.2 Hz, 2H, H_a), 8.73 (s, 1H, H_z).

^{13}C NMR: (CDCl_3 , 100 MHz) 192.72 (C_h), 165.77 (C_b), 157.74 (C_i), 151.39 (C_l), 146.73 (C_n), 137.92 (C_s , C_a , C_c , C_f), 130.91 (C_u), 127.76 (C_y , C_p , C_k , C_q , C_d , C_e), 121.46 (C_v , C_x), 116.14 (C_r , C_z), 113.16 (C_l , C_o), 105.91 (C_j , C_g), 97.70 (C_w), 68.77 (C_a), 31.93 (C_f), 29.5 (C_b , C_d , C_e), 26.16 (C_c , C_m , C_i), 22.14 (C_g), 14.16 (C_h).

The UV-vis spectrum of compound **5** (dye) in DMF exhibits the typical metal to ligand charge transfer (MLCT) transition of the Zn porphyrin complex at $\lambda_{\text{max}} = 429$ nm (Soret band), 562 nm and 604 nm (Q bands) (Figure 3). These bands show significant displacement to the longer wavelengths because of ligand binding. This is due to the instability of π electrons because of the binding to the conjugated π system of the attached ligand to the complex. The variations of substituents on the porphyrin ring in metal porphyrin complexes cause little changes to the intensity and wavelength of the absorption, the insertion or change of metal atoms into the macrocycle or protonation of two of the inner nitrogen atoms strongly change the visible absorption spectrum for these complexes.

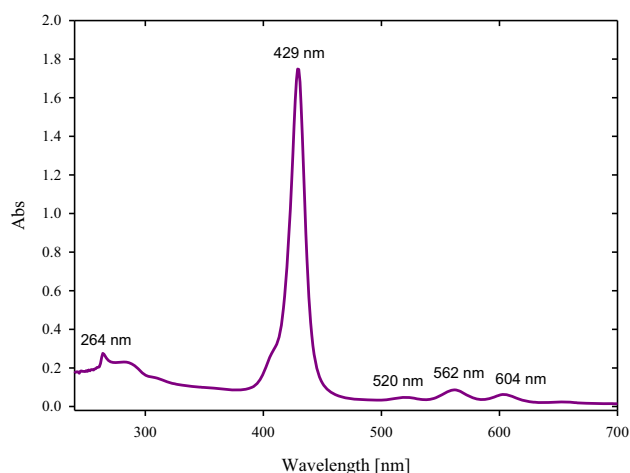


Figure 3. UV-Vis spectrum of Zn porphyrin complex (compound 5) in DMF (6×10^{-5} M) with $\epsilon = 2.9$ ($10^4 \text{ M}^{-1} \text{ cm}^{-1}$) at 429 nm.

Also, CHN analysis was carried out to determine the presence of ligand and metal in the porphyrin complex (compound 5 (dye)). CHN analysis of compound obtained: Anal. Calc. For $\text{ZnC}_{125}\text{H}_{156}\text{N}_8\text{O}_9$: C, 75.86; H, 7.89; N, 5.66. Found: C, 75.79; H, 7.96; N, 5.60%.

The Zn porphyrin complex (dye) was anchored to nanocrystalline TiO_2 film and fabricated cell exhibits a short circuit density (J_{sc}) of 11.60 and an open circuit potential (V_{oc}) of 0.65 with an efficiency of 5.33% in a DSSC. Table 1 shows the parameters of DSSC made with this Zn porphyrin complex as a sensitizer. Also, the current-voltage characteristic of this complex in DSSC was shown in Figure 4.

The high efficiency of the Zn porphyrin complex sensitized cell can be attributed to high electron injection yield and slow charge recombination rate due to bulky attachment groups that these groups avoid the aggregation of dye on TiO_2 surface. The aggregation of dye on the TiO_2 electrode surface can increase the intermolecular charge transfer between dye molecules and cause to decrease of charge transfer from dye molecules to the TiO_2 electrode surface. So it is better that we used the more π -conjugated extended compounds, with high π -delocalized substituents for enhancing the light-harvesting properties and photovoltaic performances. Also, the molar extinction

Table 1. The operation parameters of DSSCs made with a new Zn porphyrin complex as a sensitizer.

J_{sc} (mA/cm ²)	V_{oc}	η (%)	FF
11.60	0.65	5.33	0.70

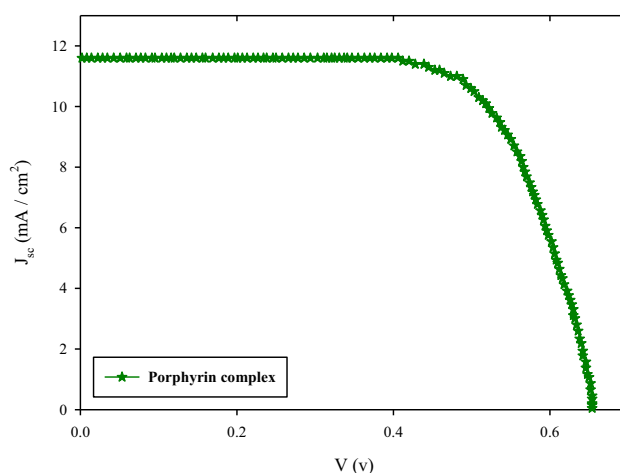


Figure 4. Photocurrent density-voltage (I - V) characteristic curves of the DSSC with this new Zn porphyrin complex as a sensitizer.

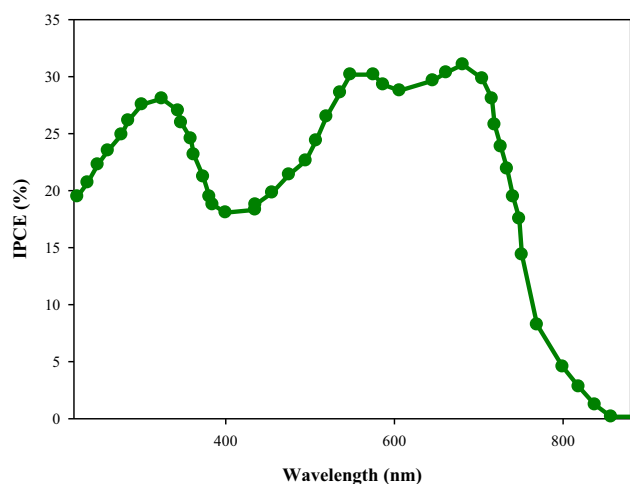


Figure 5. Photocurrent action spectra of the TiO₂ electrode sensitized by porphyrin dye (TiO₂ thickness: ~ 14μm).

coefficient of the dye molecule can affect the value of J_{sc} . Generally, a high molar extinction coefficient has a strong light-harvesting ability and gives a high J_{sc} .²⁹

The incident photon-to-current conversion efficiency (IPCE) of porphyrin dye is shown in Figure 5. The IPCE curve of the cell sensitized with porphyrin dye showed the highest plateau from 550 to 700 nm, with a maximum at 700 nm. The IPCE value of the DSSC based on dye is due to π -conjugation elongation and the value of electron injection yield. So the high IPCE value of DSSC could be attributed to the increased electron injection yield on TiO₂ film.

4. Conclusions

In summary, a new Zn porphyrin complex was synthesized by a multistep procedure for dye-sensitized solar cell applications. The Zn porphyrin complex anchored to the TiO₂ surface acts as a photosensitizer in a nanocrystalline dye-sensitized solar cell. Furthermore, the photoelectrochemical properties of complex were investigated. A solar-to-electric conversion efficiency of 5.33% is achieved with this Zn porphyrin dye under the standard AM 1.5 conditions.

Supplementary Information (SI)

¹HNMR and ¹³CNMR spectra data is available at www.ias.ac.in/chemsci.

Acknowledgements

The support of this work by the University of Isfahan is acknowledged.

References

- Ito S, Murakami T N, Comte P, Liska P, Grätzel C, Nazeeruddin M K and Grätzel M 2008 Fabrication of thin-film dye-sensitized solar cells with solar to electric power conversion efficiency over 10% *Thin Solid Films* **516** 4613
- Fateminia S M A, Yazdani-Rad R, Ebadzadeh T and Ghoshghai S 2011 Effect of dispersing media on microstructure of electrophoretically deposited TiO₂ nanoparticles in dye-sensitized solar cells *Appl. Surf. Sci.* **257** 8500
- En Mei J, Kyung-Hee P, Ju-Young P, Jae-Wook L, Soon-Ho Y, Xing G Z, Hal-Bon G, Sung-Young C, John G F and Tae-Young K 2013 Preparation and characterization of Chitosan binder-based TiO₂ electrode for dye-sensitized solar cells *Int. J. Photoenergy* **2013** 1
- Jin E M, Park K H, Yun J J, Hong C K, Hwang M J, Park B K, Kim K W and Gu H B 2010 Photovoltaic properties of TiO₂ photoelectrode prepared by using liquid PEG-EEM binder *Surf. Rev. Lett.* **17** 15
- Park K H, Gu H B, Jin E M and Dhayal M 2010 Using hybrid silica-conjugated TiO₂ nanostructures to enhance the efficiency of dye-sensitized solar cells *Electrochim. Acta* **55** 5499
- Tan B and Wu Y 2006 Dye-sensitized solar cells based on anatase TiO₂ nanoparticle/nanowire composites *J. Phys. Chem. B* **110** 15932
- Oregan B B and Grätzel M 1991 A low-cost, high-efficiency solar cell based on dye-sensitized colloidal TiO₂ films *Nature* **353** 737
- Wang Q, Campbell W M, Bonfantani E E, Jolley K W, David L, Walsh P J, Gordon Humphry-Baker K R, Nazeeruddin M K and Grätzel M 2005 Efficient light harvesting by using green Zn-porphyrin-sensitized nanocrystalline TiO₂ films *J. Phys. Chem. B* **109** 15397
- Ball J M, Davis N K S, Wilkinson J D, Kirkpatrick J, Teuscher J, Gunning R, Anderson H L and Snaith H J 2012 A panchromatic anthracene-fused porphyrin sensitizer for dye-sensitized solar Cells *RSC Adv.* **2** 6846
- Campbell W M, Jolley K W, Wagner P, Wagner K, Walsh P J, Gordon K C, Schmidt-Mende L, Nazeeruddin M K, Wang Q and Grätzel M 2007 Highly efficient porphyrin sensitizers for dye-sensitized solar cells *J. Phys. Chem. C* **11** 11760
- So S, Fan S Q, Choi H, Kim C, Cho N, Song K and Ko J 2010 Stepwise cosensitization through chemically bonding organic dye to CdS quantumdot-sensitized TiO₂ electrode *Appl. Phys. Lett.* **97** 263506 (1–3)
- Kim J Y, Lee K, Coates N E, Moses D, Nguyen T Q, Dante M and Heeger A J 2007 Efficient tandem polymer solar cells fabricated by all-solution processing *Science* **317** 222
- Mojiri-Foroushani M, Dehghani H and Salehi-Vanani N 2013 Enhancement of dye-sensitized solar cells performances by improving electron density in conduction band of nanostructure TiO₂ electrode with using a metalloporphyrin as additional dye *Electrochim. Acta* **92** 315
- Lan C M, Wu H P, Pan T Y, Chang C W, Chao W S, Chen C T, Wang C L, Lin C Y and Diao E W G 2012 Enhanced photovoltaic performance with co-

- sensitization of porphyrin and an organic dye in dye-sensitized solar cells *Energy Environ. Sci.* **5** 6460
15. Wang X F and Tamiaki H 2010 Cyclic tetrapyrrole based molecules for dye-sensitized solar cells *Energy Environ. Sci.* **3** 94
 16. Walter M G, Rudine A B and Wamser C C 2010 Porphyrins and phthalocyanines in solar photovoltaic cells *J. Porphyrins Phthalocyanines C* **14** 759
 17. Dong H, Zhou X and Jiang C 2012 Molecular design and theoretical investigation on novel porphyrin derivatives for dye-sensitized solar cells *Theor. Chem. Acc.* **131** 1102 (1–11)
 18. Yella A, Lee H W, Tsao H N, Yi C Y, Chandiran A K, Nazeeruddin M K, Diau E W G, Yeh C Y, Nazeeruddin S M and Grätzel M 2011 Porphyrin-sensitized solar cells with cobalt (II/III)-based redox electrolyte exceed 12% efficiency *Science* **334** 629
 19. Karthikeyan S and Jin Yong L 2013 Zinc-porphyrin based dyes for dye-sensitized solar cells *J. Phys. Chem. A* **117** 10973
 20. Mai C L, Huang W K, Lu H P, Lee C W, Chiu C L, Liang Y R, Diau E W G and Yeh C Y 2010 Synthesis and characterization of diporphyrin sensitizers for dye-sensitized solar cells *Chem. Commun.* **46** 809
 21. Hayashi S, Tanaka M, Hayashi H, Eu S, Umeyama T, Matano Y, Araki Y and Imahori H 2008 Naphthyl-fused π -elongated porphyrins for dye-sensitized TiO₂ Cells *J. Phys. Chem. C* **112** 15576
 22. Chongjun J, Ningning Z, Kuo-Wei H, Peng W and Jishan W 2011 Perylene anhydride fused porphyrins as near-infrared sensitizers for dye-sensitized solar cells *Org. Lett.* **13** 3652
 23. Arteaga D, Cotta R, Ortiz A, Insuasty B, Martin N and Echegoyen L 2015 Zn(II)-porphyrin dyes with several electron acceptor groups linked by vinyl-fluorene or vinyl-thiophene spacers for dye-sensitized solar cells *Dyes Pigm.* **112** 127
 24. Mohr B, Enkelmann V and Wegner G 1994 Synthesis of alkyl- and alkoxy-substituted benzils and oxidative coupling to tetraalkoxy phenanthrene-9,10-diones *J. Org. Chem.* **59** 635
 25. Adler A, Long F R and Kampass F 1970 On the preparation of metalloporphyrins *J. Inorg. Nucl. Chem.* **32** 2443
 26. Kruper W J, Chamberlin T A and Kochanny M 1989 Regiospecific aryl nitration of meso-substituted tetraarylporphyrins: a simple route to bifunctional porphyrins *J. Org. Chem.* **54** 2753
 27. McNamara W R, Snoeberger R C, Li G, Schleicher J M, Cady C W, Poyatos M, Schmuttenmaer C A, Crabtree R H, Brudvig G W and Batista V S 2008 Acetylacetonate anchors for robust functionalization of TiO₂ nanoparticles with Mn(II)-terpyridine complexes *J. Am. Chem. Soc.* **130** 14329
 28. Jiang Y W, Wu N, Wu H H and He M Y 2005 An efficient and mild CuI/l-proline-catalyzed arylation of acetylacetone or ethyl cyanoacetate *Synlett* **2005** 2731
 29. Siu C H, Ho C L, He J, Chen T, Cui X, Zhao J and Wong W Y 2013 Thiocyanate-free ruthenium(II) cyclometalated complexes containing uncommon thiazole and benzothiazole chromophores for dye-sensitized solar cells *J. Organomet. Chem.* **748** 75